چکیده فارسی

مطالعه عددی اثر شکل تاج پیستون برروی فرآیند احتراق و آلایندگی موتورهای دیزلی پاشش مستقیم

گروه مهندسی مکانیک، دانشکده فنی، دانشگاه ارومیه

صمد جعفرمدار و مجتبی خانبابازاده

در مقاله حاضر یک مطالعه عددی به منظور بررسی اثر شکل تاج پیستون بر روری فرایند احتراق و آلایندگی موتور دیزلی پاشش مستقیم ارائه شده است. پارامترهای مختلف فرایند احتراق، آلایندگی و میدان جریان داخل سیلندر از جمله تغییرات فشار، دمای متوسط، میدان سرعت، نرخ گرمای آزاد شده، آلایندگی و نحوه شکل‌گیری احتراق داخل سیلندر در سه حالت مختلف شکل تاج پیستون مورد بررسی قرار گرفته است. با توجه به نتایج به دست آمده می‌توان گفت که شکل تاج پیستون اثرات قابل توجهی بر روری فرایند احتراق و آلایندگی دارد. با مقایسه نتایج می‌توان نتیجه‌گیری کرد که مخفظه احتراق امگاشکل (reentrant combustion chamber) با ارتفاع برامدگی زیاد به دلیل تشدید حرکات چرخشی (swirl and tumble flow) و احتراق دماپائین نسبت به دیگر حالت‌ها مقدار آلاینده‌ای Soot و NO_x کمتری دارد. هم‌چنین نشان داده شده است که عمق محفظه احتراق یکی از پارامترهای موثر در کنترل آلاینده‌هاست. نتایج به دست آمده از این مدل برای حالت استوانه‌ای با نتایج تجربی مقایسه شده و توافق خوبی را نشان می‌دهد. در حالت کلی می‌توان گفت که تاج پیستون امگاشکل بهترین انتخاب برای موتورهای دیزلی پاشش مستقیم می‌باشد ولی باید با مشخصات سیستم پاشش سوخت نیز مطابقت داشته باشد.

واژگان کلیدی: هندسه محفظه، مدلسازی، آلاینده، فرایند احتراق، چرخش افقی، چرخش عمودی

Conclusions

This study has revealed that flame behavior is strongly dependent on combustion chamber geometry. The reentrant chamber prevents the flame from spreading over the squish region and fast mixing, makes a great reduction in exhaust soot by increasing swirl and tumble. Also because of the low temperature in the cylinder, the chamber is confirmed from NO_x viewpoint. The result of this model for the NOx emission and pressure cylinder at the cylindrical combustion chamber are compared with the corresponding experimental data, and prove to be in good agreement. But it should be noticed that the nozzle position is in strict relation with soot production. Combustion chamber optimization is not sufficient by itself and accurate optimization in injector position by combustion chamber is needed to have a large reduction in emissions.

References

1. Takatsuki , T., et al., "Development of a New Low-Pollution and High-Output Combustion Chamber," Journal of JSAE, Vol. 48, NO. 10, p. 36, 1994.
2. Zhang, L., et al., "In-Cylinder Flow Measurement by Cross-Correlation Method," Trans of JSAE, Vol. 25, No. 4, p. 10, 1994.
3. Tabata, T., et al., "Numerical Calculation of Spray Mixing Process in a D.I.Diesel Engine and Comparison with Experiments," SAE Paper 950853.
4. Konno, M., hikahisa, T., and Murayama, T., "Reduction of Smoke and NO_x by Strong Turbulence Generated During the Combustion Process in D.I.Diesel Engine," SAE 920467.
5. Tow, T. C., Piperpoint, D. A., and Reitz, R. D., "Reducing Particulate and NO_x Emissions by Using Multiple Injections in A Heavy Duty D.I.Diesel Engine," SAE Paper 950897.
6. Bai-fu Lin, Masaru Ogura, "A New Multi-Impingement-Wall Head Diffusion Combustion System (NICS-MH) of a DI Diesel Engine - The Effect of Combustion Chamber Geometry," SAE Paper 951792.
7. Long Zhang, Takahiro Ueda, Toshiaki Takatsuki and Katsuhiko Yokota, "A Study Effects of Chamber Geometries on Flame Behavior in a DI Diesel Engine," SAE Paper 952515.
8. Shioji, M., et al., "An Analysis of Diesel Engine Flame by Picture Processing," JSME Int Journal, Series 2, Vol. 32, No. 3, 1989.
9. Yamaguchi, I., et al., "An Analysis of High Speed Combustion Photographs for D.I. Diesel Engine with High Pressure Fuel Injection," SAE Paper 901577.
10. Cox, R., and Cole, J., "Chemical Aspects of the Auto Ignition of Hydrocarbon-Air Mixtures," SAE, 1994.
11. Fisch, A., Read, A., Affleck, W., and Haskell, W., "The Controlling Role of Cool Flames in Two-Stage Ignition," Combustion Flame, Vol. 13, pp. 39-49, 1969.
12. Halstead, M., Kirsch, L., Prothero, A., and Quinn, O., "A Mathematical Model for Hydrocarbon Auto-Ignition at High Pressures," Proc. Royal Society of London, A246, pp. 515-538, 1975.
13. Halstead, M., Kirsch, L., and Quinn, C., "The Autoignition of Hydrocarbon Fueld at High Temperatures and Pressures - Fitting of A Mathematical Model," Combustion Flame, Vol. 30, pp. 45-60, 1977.
14. Zeldovich, Y. B., Sadovnikov, P. Y., and Frank-Kamenetskii, D. A., Oxidation of Nitrogen in Combustion, Translation by M. Shelef, Academy of Sciences of USSR, Institute of Chemical Physics, Moscow-Leningrad, 1947
15. Bogensperger, M., "A Comparative Study of Different Calculation Approaches for the Numerical Simulation of Thermal NO Formation," Diss. U. Graz, 1996.
16. Heywood, J. B., Internal Combustion Engine Fundamentals, McGraw-Hill Book Company, Second Series, 1988.
17. Warnatz, J., and Maas, U., Technische Verbrennung, Physikalisch-Chemische Grundlagen, Modelbildung, chadstoffentstehung, Springer Verlag Berlin Heidelberg, 1993.
18. Tatschl, R., Pachler, K., Fuchs, H., and Almer, W., "Multidimensional Simulation of Diesel Engine Combustion - Modeling and Experimental Verification," Proceedings of the Fifth Conference 'The Working Process of the Internal Combustion Engine', Graz, Austria, 1995.
19. Tesner, P. A., Snegriova, T. D., and Knorre, V. G., "Kinetics of Dispersed Carbon Formation," Combustion and Flame, Vol. 17, pp. 253-260, 1971.
20. Magnussen, B. F., and Hjertager, B. H., "On Mathematical Modeling of Turbulent Combustion with Special Emphasis on Soot Formation and Combustion," Sixteenth International Symposium on Combustion, Pittsburgh, The Combustion Institute, 1977.
21. Liu, A. B., and Reitz, R. D., "Modeling the Effects of Drop Drag and Break-up on Fuel Sprays," SAE 930072.
22. Gosman, A. D., and Ioannides, E., "Aspects of Computer Simulation of Liquid-Fueled Combustors," AIAA, pp. 81-323, 1981.
23. Naber, J. D., and Reitz, R. D., "Modeling Engine Spray/Wall Impingement," SAE- 880107.
24. Wachters, L. H. J., and Westerling, N. A. J., "The Heat Transfer from a hot Wall to Impinging Water Drops in Speroidial State," Chem. Eng. Sci., Vol. 21, pp.737-743, 1966.
25. Dukowicz, J. K., "Quasi-Steady Droplet Change in the Presence of Convection, Informal Report Los Alamos Scientific Laboratory," LA7997-MS, 1980.
26. Ranz, W. E., and Marshall, W. R., "Evaporation from Drops," Chem. Eng. Prog. Vol. 48, pp. 141-146, 173-180, 1952.
27. Bose, A. K., and Pei, C. T., "Evaporation Rates in Spray Drying," Can. J. Chem., Vol. 42, p. 252, 1964.
28. Pirouzpanah, V., et al., "Reduction of Pollutants Emissions of OM355 Diesel Engine to Euro2 by Converting to Dual Fuel Engine (Diesel+Gas)," Proceeding of first Conference of Automotive Fuel to CNG, pp. 84-94, Tehran, Iran, Jun 2003.

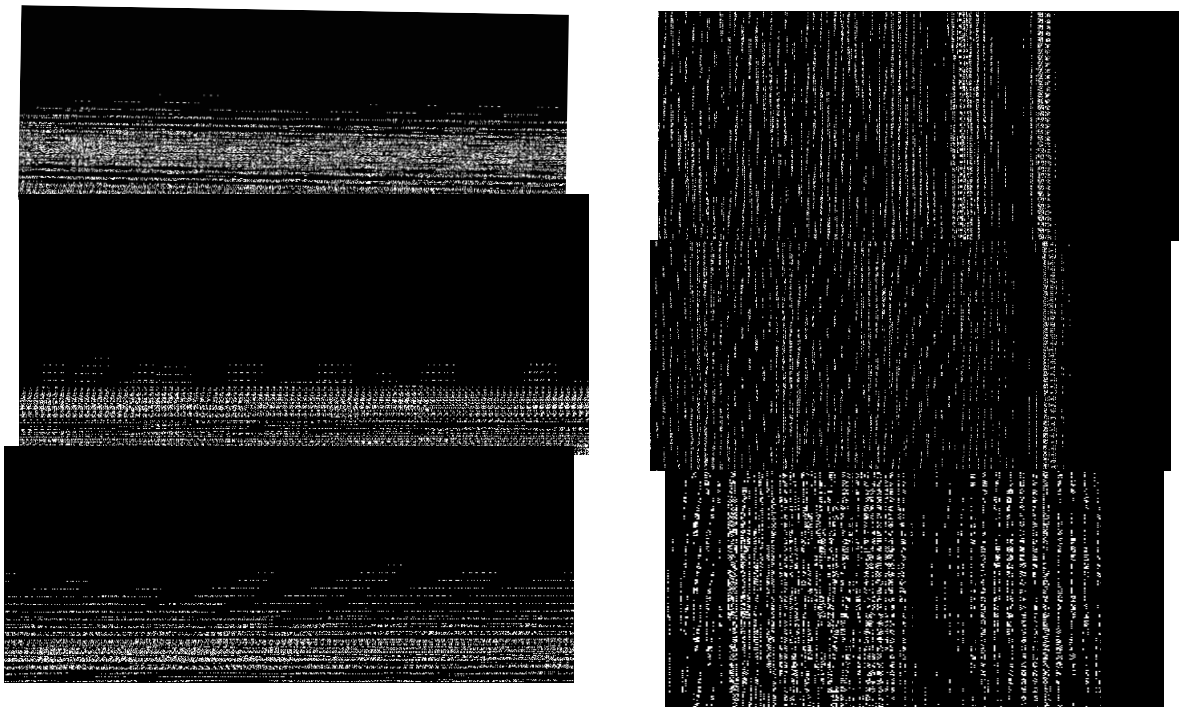

(a) **(b)**

Figure 20. Tumble at a) 360 and b) 390 deg of CA for cylinder, omega1, omega2 models respectively

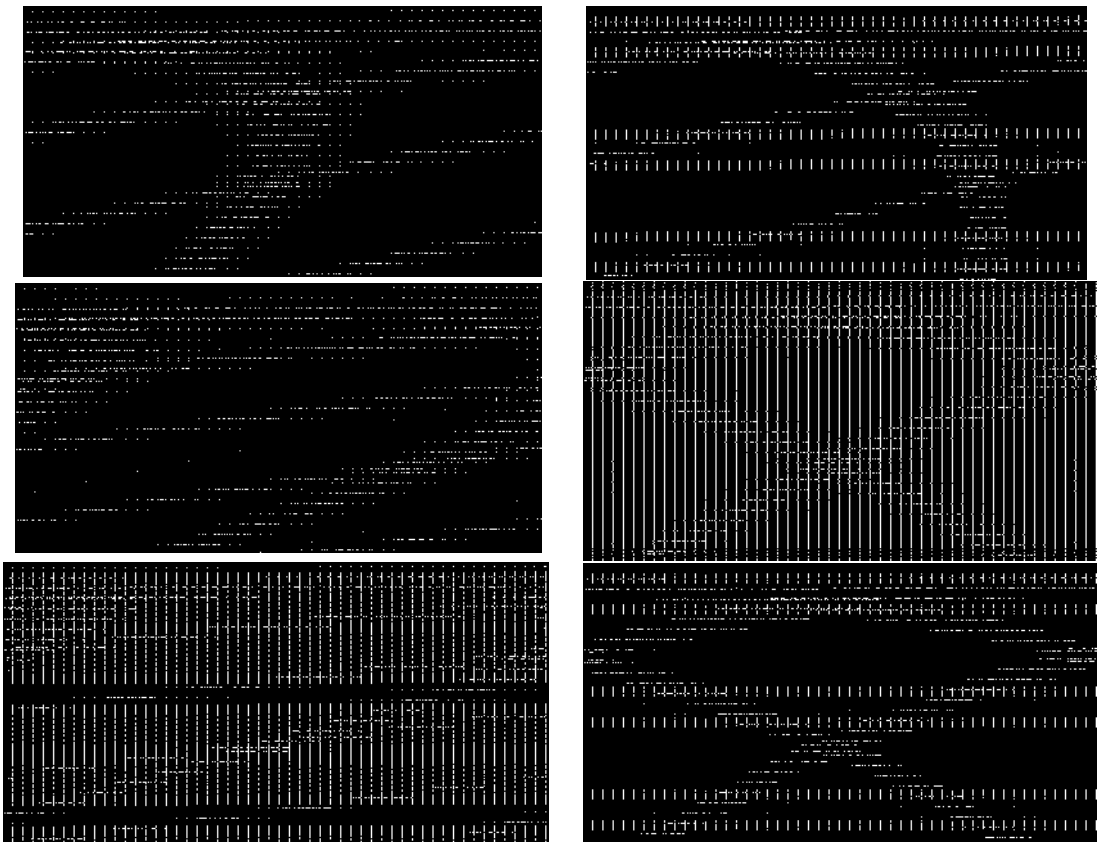

(a) **(b)**

Figure 21. Swirl vectors at a) 360 and b) 390 deg of CA for cylinder, omega1, omega2 models respectively

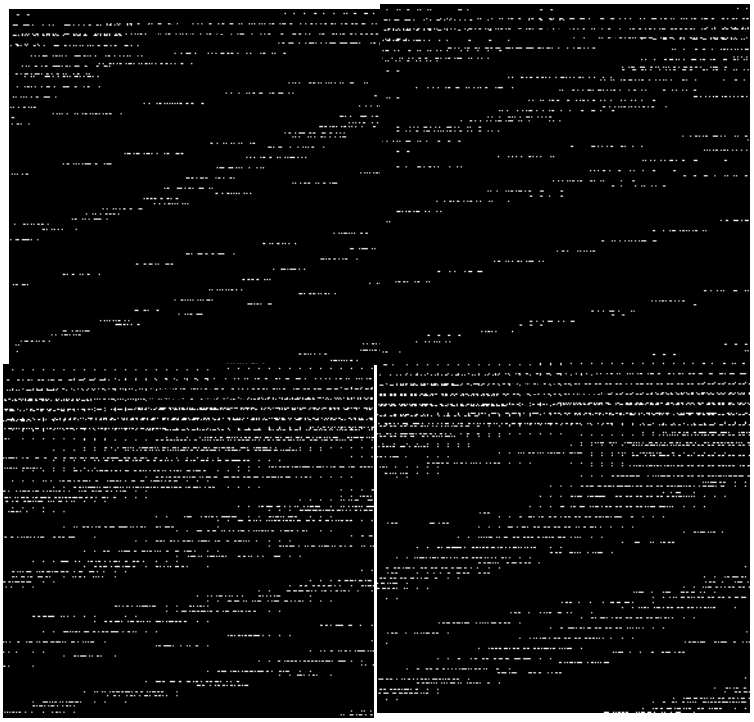

Figure 18. Contours of flame distribution at (360, 370, 380 and 390 ^{o}CA) for omega2 model

Figure 19. Contours of soot mass fraction at (360, 370, 380 and 390 ^{o}CA) for omega2 model

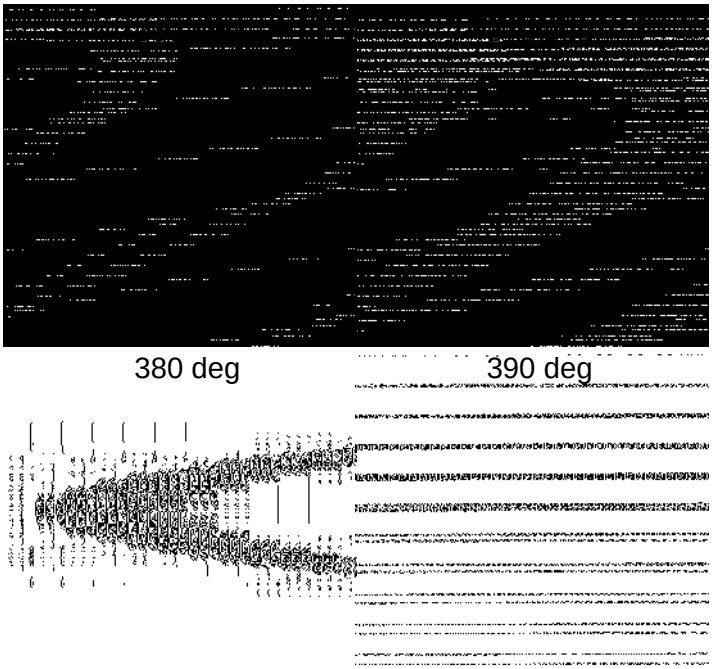

Figure 16. Contours of flame distribution at (360, 370, 380 and 390 ^{o}CA) for omega1 model

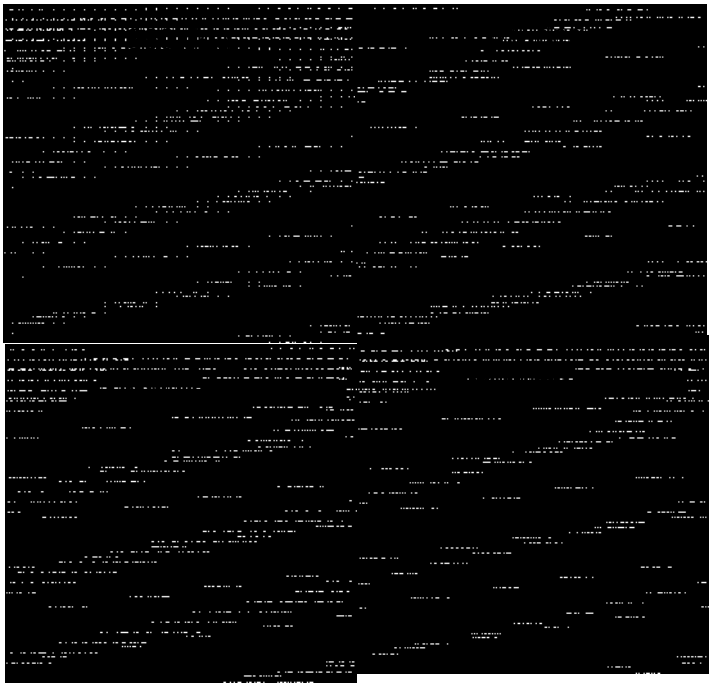

Figure 17. Contours of soot mass fraction at (360, 370, 380 and 390 ^{o}CA) for omega1 model

mixing due to swirl motion might enhance soot oxidation. Another reason for soot formation is fuel impinging (not shown), which is more important at the omega1. A consideration of Fig.20 and Fig.21 reveals that tumble and swirl in omega shape piston head is larger than in the cylindrical piston head (however the difference in swirl of all models is little at 360deg CA). So as a further look at Fig.15, Fig.17, Fig.19, Fig.20 and Fig.21 show, where tumble and swirl is large and there is no impinging fuel, smoke reduction will increase and vice versa. Also the large mean soot mass fraction for the Omega1 and Omega2 models is related to the spray angle, which causes impingement to come up, so when piston moves to the bottom, the volume of the squish area becomes large and flame/fuel becomes richer than air mass fraction resulting in an increased smoke emission. So it is clearly obvious that the role of air swirl and tumble is a significant factor in soot reduction. Large swirl and tumble means that turbulence is large and it results in air/fuel ratio increase as well as considerable soot reduction. Generally it is obvious that Omega2 is the better than the others from the emission production viewpoint, however, further optimization is needed to reach the best efficiency and the lowest exhaust emissions by means of governing a balancing between injection angle, swirl and tumble.

Figure 14. Contours of flame distribution at (360, 370, 380 and 390 ^{o}CA) for cylinder model

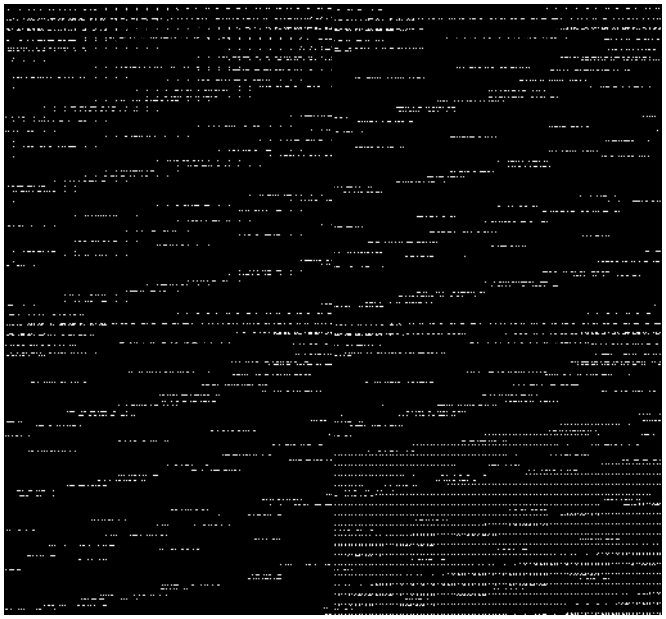

Figure 15. Contours of soot mass fraction at (360, 370, 380 and 390 ^{o}CA) for cylinder model

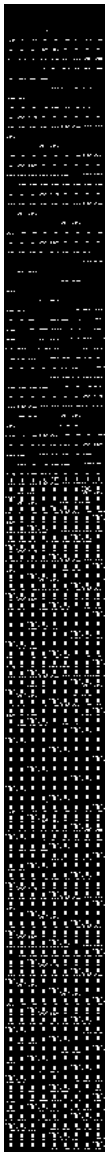

Figure 13. Contours of NO_x mass fraction at (400 ^{q}CA) for the Cylinder, Omega1and Omega2 respectively

The other important parameters to discuss are the flame Velocity, and flame distribution in the chamber. It is well known that for further smoke reduction, it is important to achieve fast flame motion during diffusion combustion, and desirable fuel/flame distribution inside and outside the chamber simultaneously.

Fig.14, to Fig.19 shows flame distribution and soot mass fraction contours for all models at four positions of piston, which completely confirms the results.

Also in further consideration the relationship between flame movement and smoke emissions is shown in figures 14 to19, which reveales that smoke emission is larger in Omega1 and Cylinder models than Omega2 at each degree of crank angle. But comparing the variation of smoke emission between Omega1 and the cylinder model is not easy because of the irregularity of the changes in soot production in these models. However, a look again at Fig.7 reveals that soot production of the Cylinder model is generally lowers than that in other models. The reason lies in the fact that if larger flame/fuel spreads over narrow clearance in the squish region earlier when the piston is near the TDC, cooling effect of the wall, weak air tumble, as well as swirl occur in the cylinder (This is different from initial swirl at the start of calculations). In other words, after combustion, weak swirl in this region will cause large soot formations and poor oxidation of the formed soot. In addition, the swirling motion of the gas phase plays an important role in mixing process between fuel and air, and between partially oxidized product (soot) and air. When there exists a high swirling motion, liquid fuel and fuel vapor (with higher density than the ambient gases) in the core region of sprays tend to move from the inner region to the outer region where fresh air is available (centrifugal-forced-induced-stratification). In contrast, the hot (low density) combustion products move towards the inner region. Thus, it is expected that the induced secondary

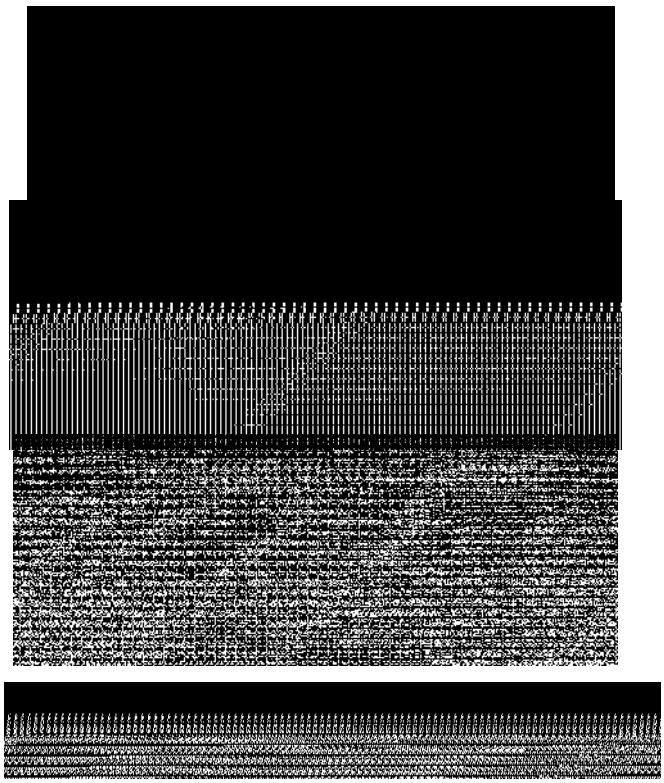

Figure 11. Contours of soot mass fraction at TDC (360 ^{q}CA) for each model respectively (Cylinder, Omega1and Omega2)

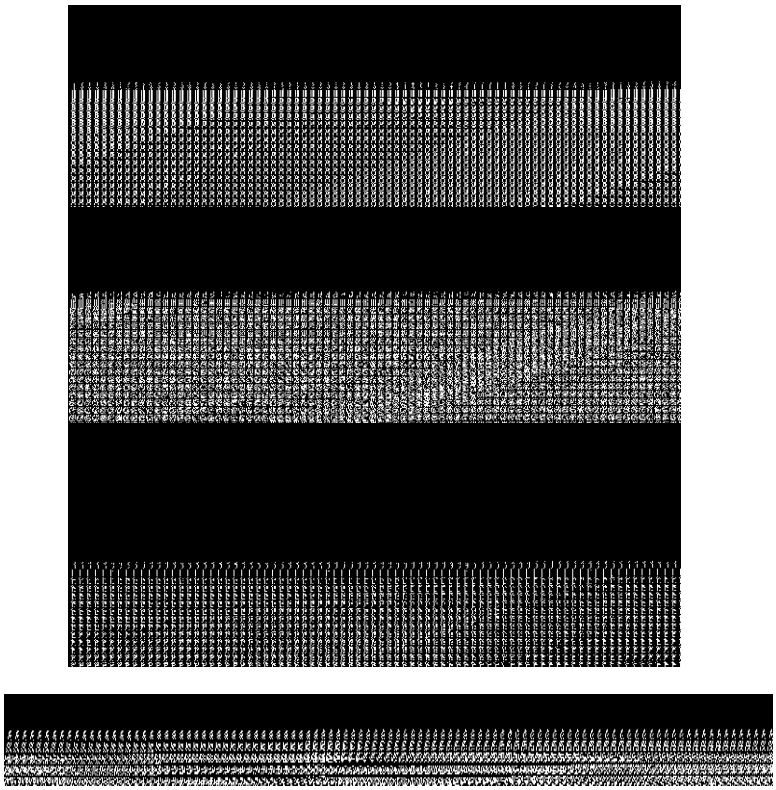

Figure 12. Contours of soot mass fraction at (370 ^{q}CA) for each model respectively (Cylinder, Omega1and Omega2)

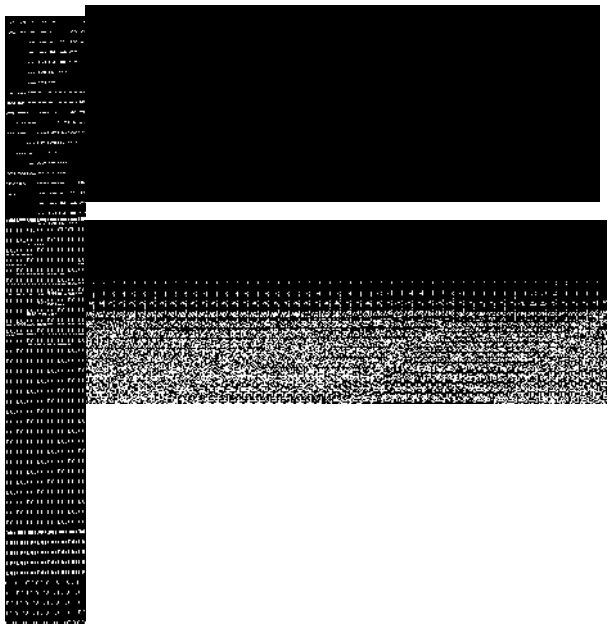

Figure 9. Contours of O_2 mass fraction at (360 ^{o}CA) for each model respectively (Cylinder, Omega1and Omega2)

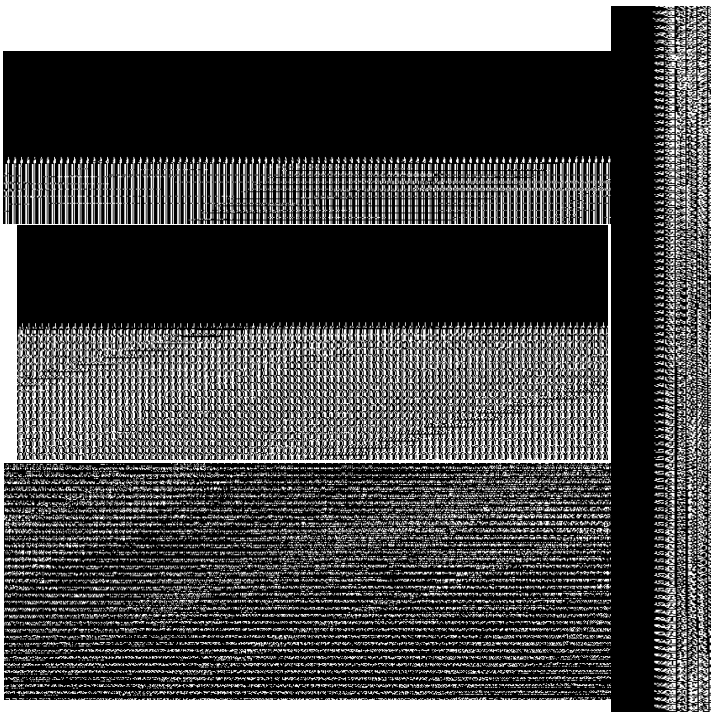

Figure 10. Contours of NO_x mass fraction at (360 ^{o}CA) for each model respectively (Cylinder, Omega1and Omega2)

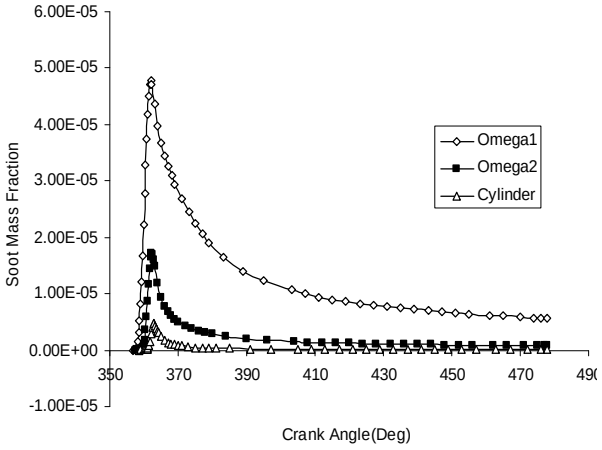

Figure 7. Calculated soot mass fraction versus crank angle

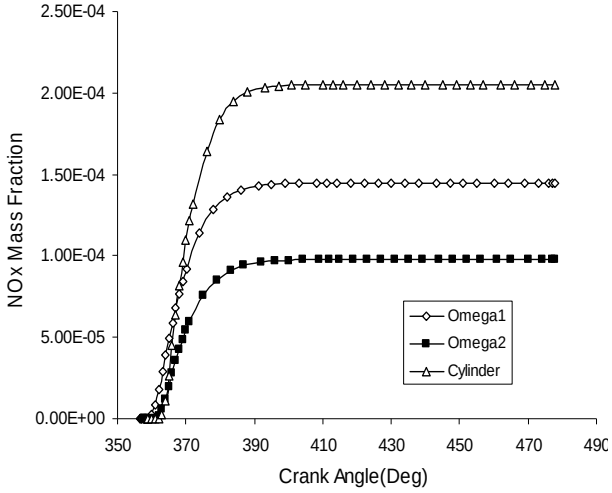

Figure 8. Calculated NOx mass fraction versus crank angle

For the above described reason, and with the comparison between Fig.9 and Fig.10, it is clear that the NOx mass fraction is the smallest for the Omega2 model, whereas cylindrical model has the maximum value of NOx. The other remaining model has the amount of NO_x between the cylindrical and the Omega2 models. Contrary to the NO_x mass fraction, the amount of soot mass fraction at every Crank angle is the lowest for the cylindrical model and highest for the Omega1 model.

As an example, Fig.9, Fig.10 and Fig.13 show O_2 and NO_x mass fraction contours for each model at 360 and 400 CA respectively.

In addition, the area where the equivalence ratio is higher than 3 and the temperature is approximately between 1600 K and 2000 K is the Soot formation area. Also there are two factors that control the soot oxidation: temperature and availability oxidizer(air). Therefore, the mass fraction of soot is strongly associated with O_2 mass fraction or accurately equivalent Fuel/Air ratio and local temperature. In other words, where Fuel/Air ratio and local temperature is high, the probability of soot formation increases. Fig.9, Fig.11 and Fig.12 confirm this fact. The cylindrical shape, because of its high temperature zone and fairly good mixing (medium swirl), and the omega2 shape, because of its medium temperature zone and intense mixing (high swirl ratio), have less soot emission than the omega1 shape.

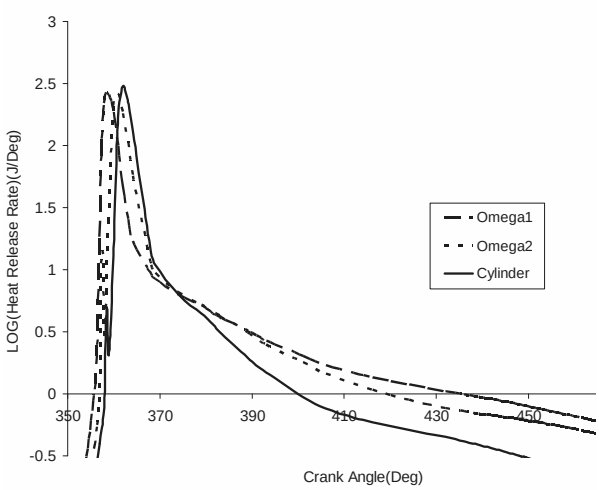

Figure 5. Calculated heat release rate versus crank angle

In Fig.6, the experimental pressure cylinder and the NOx emission for the cylindrical shape combustion chamber are compared with the corresponding experimental data [28],which show good agreement.

Fig.7 and 8 show the predicted soot and NOx emissions variation vs. crank angel. As indicated, the general trends of reduction in NOx and increase in soot can be observed (trade- off soot and NOx). As a whole, it can be seen that the area where the equivalence ratio is close to 1, the temperature is higher than 2000 K and the O_2 is available, is the NOx formation area.

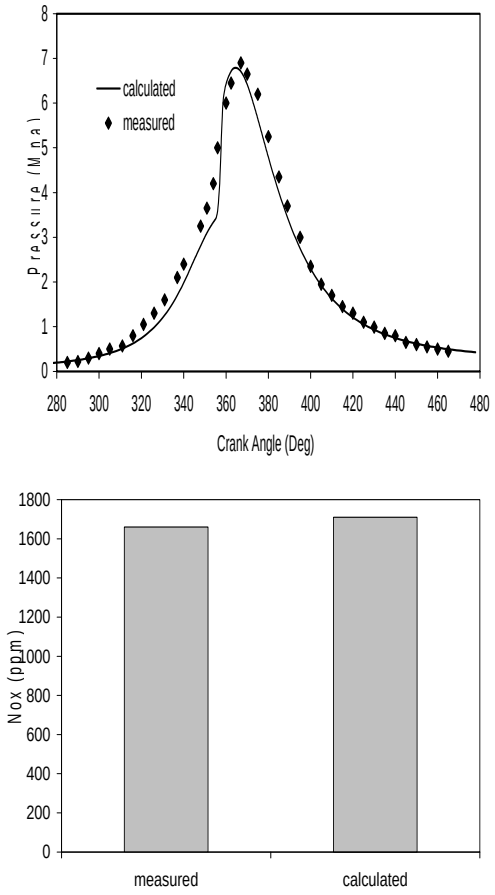

Figure 6. Comparison of experimental data and numerical for the cylindrical geometry chamber [28]

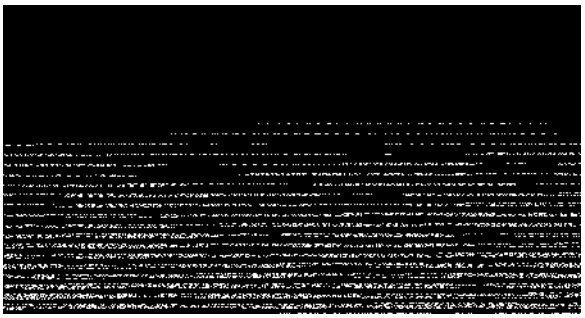

Figure 2. Outline of the computational mesh at 12 degree BTDC for a quarter of the engine combustion chamber

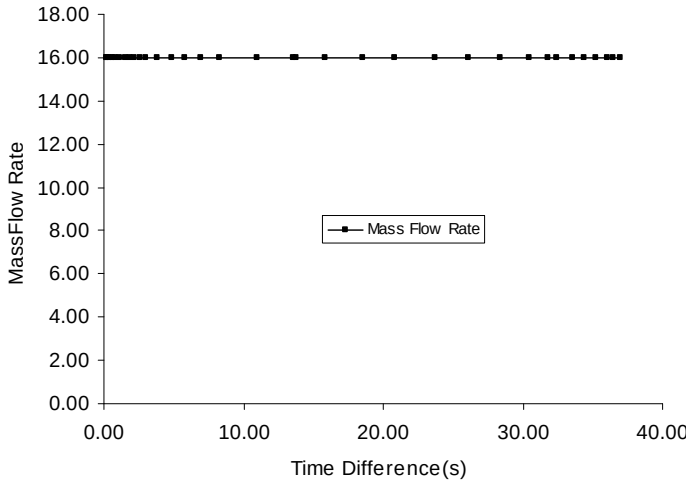

Figure 3. Injection rate schemes

The results are discussed in the next section.

Results and discussion

As previously described, the model was computed for a three combustion chamber shape, and the results obtained are as follows:

Fig.4 shows time histories of in-cylinder temperature, and it is clear that, because of the retard combustion and the lack of stoichiometric mixture zones in the cylinder, the omega2 shape has the lowest temperature.

Heat release rate data are presented in Fig.5. The fact that the combustion process proceeds in two phases, namely premixed and diffusion, is clear in this figure. Also because of the fast mixture formation and high temperature in cylinder, omega shape has the least ignition delay.

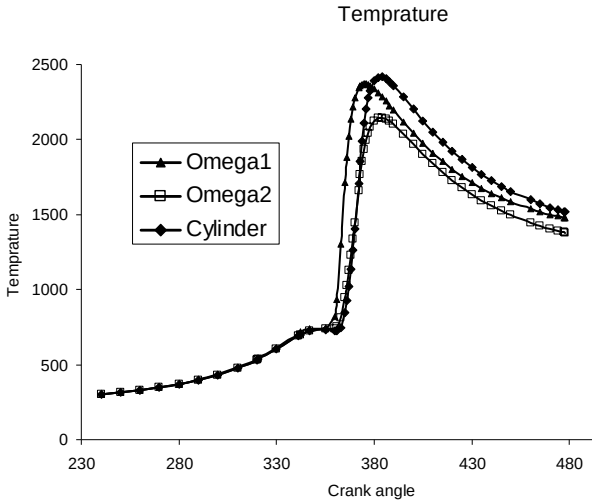

Figure 4. Calculated temperature versus crank angle

note that usually $\overline{u_i u_j} \neq 0$ when $\partial U_i / \partial x_j > 0$ so that in most flows P > 0; G is the production (or destruction) of k by body force; ε - dissipation of k into heat by the action of viscosity (Note $\varepsilon > 0$ always); D - diffusive transport of k (viscous, by fluctuating velocity and pressure, respectively).

To predict how combustion chamber geometry affects the combustion process, three models (omega1, omega2, cylinder) have been defined, whose characteristics have been specified in Table.1 and Fig.1. Omega1 and Omega2 models are related to chamber in Fig1.a and the next represents the chamber in the shape of a cylinder (Fig1.b). General specification of engine also has been given in Table.2.

Table 1. Geometrical specifications of combustion chamber

	Omega1	Omega2	Cylinder
Tm (mm)	9	6	12.65
Dr(mm)	86.61	86.61	
Db(mm)	79.21	79.21	89.29
R2(mm)	3.85	3.85	
R3(mm)	9.0	9.0	
R4(mm)	4.92	4.92	4.92
R5(mm)	5.91	5.91	
S2(mm)	0.39	0.39	
Bowl volume (mm^3)	1159.04 $\times 10^{-2}$	1114.43 $\times 10^{-2}$	1159.81 $\times 10^{-2}$

Table 2. Engine specifications and conditions

piston course (mm)	150.0
Rod length (mm)	280.0
Compression ratio	16:1
Volume clearance (cm^3)	127.814
Number of nozzle orifice $\times$ hole diameter (mm)	4 $\times$ 3.1
Engine speed (rpm)	1400
Spray angle between piston head axes and nozzle hole axes (degree)	70
Combustion chamber shape	Omega
Initial pressure (bar)	1
Initial temperature (K)	301
Inlet air temperature	301
Primary Swirl (rpm)	1500
Intake valve closure (degree)	-120 btdc
Fuel	Standard diesel fuel
Injection fuel temperature(K)	353

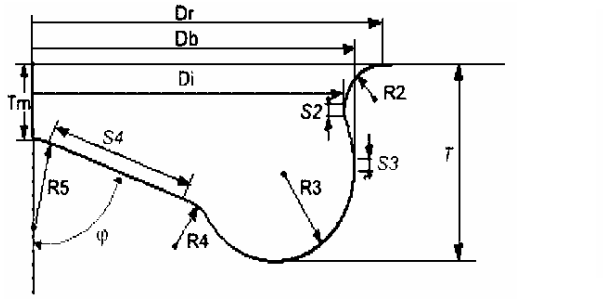

(a) **(b)**

Figure 1. Combustion chamber geometry

The injector used in computations includes 4 nozzles and 3.1mm hole diameter. The injection rate scheme is the same for all models as Fig.3.

The computational mesh developed by AVL FIRE V8.3 represents a quarter of the OM355 engine combustion chamber (i.e., a 90 degree sector) for computational efficiency, since the injector has four injection holes and all computations are carried out at 1400 rpm and at full load (the worst operation point with respect to emission). There were 68 cells in the redial direction, 15 cells in the azimuthal direction. The number of cells in the axial direction is variable so as to avoid formation of negative volume cells during the compression process. This mesh resolution, as can be seen in Fig.2, gives adequate accuracy in computations.

$$
\begin{aligned}
&We \le 50 && d_1 = d_0 \\
&50 \le We \le 300 && d_1 = d_0 \cdot f(We_{d,in}) \qquad (1)\\
&We > 300 && d_1 = 0.2 \cdot d_0
\end{aligned}
$$

The reflection angle may vary within 0< < 5 degrees.

The droplet heat-up and evaporation process is based on a model originally derived by Dukowicz [25]. Heat and mass transfer coefficients are set-up according to the model physics, but for fine tuning and matching with the experimental data, two adjustment parameters (E1, E2) for the heat and mass transfer coefficients are provided for this model.

In the evaporation model of Dukowicz [25], it is considered that the droplet is evaporating in a non-condensable gas. So it uses a two-component system in the gas-phase composed of the vapor and the non-condensable gas, even though each component may consist of a mixture of different species.

For spherical droplets, the heat flux can be obtained from heat transfer coefficient correlations. The Nusselt number Nu is obtained from the following correlation proposed by Ranz and Marshall [26] for single droplets, and is shown to be applicable to certain types of sprays by Bose and Pei [27]

$$Nu = 2 + 0.6\,\mathrm{Re}^{1/2}\,\mathrm{Pr}^{1/3} \qquad (2)$$

Model description

The numerical models used are based on the standard hydrocarbon auto-ignition mechanism combustion model developed by Cox, et al [10]; Fisch, et al [11]; Halstead, et al [13] for the simulation of gas/wall heat transfer, high temperature combustion, species transport, ignition, turbulent combustion, and pollutant formation of hydrocarbon fuel, air, and residual (exhaust) gas as discussed previously. Eddy Breakup model was developed as the combustion model together with the active turbulence controlled combustion model (based on Magnussen's formulation). The reaction time scale in this model is calculated in relation to the turbulence of kinetic energy k, and its dissipation rate ε. Zeldovich model was used as NO model and Kennedy-Hyroyasu-Magnussen as soot formation model.

The submodels for spray breakup, ignition and combustion used in this study are those discussed in the work of Liu, A.B. and Reitz, R.D [21]. These models were applied to simulate single and multiple injection combustion diesel engines under a wide range of operating conditions, and good agreement between predictions and measurements were obtained [22]. The wall interaction submodel in the mentioned model is considered as Walljet1. For the spray breakup model, the Wave model was applied.

The k-ε model is the most widely used turbulence model, particularly for industrial computations and has been implemented into most CFD codes. It is generally accepted that the k-ε model usually yields reasonably realistic predictions of major mean-flow features in most situations. Hence $k-\varepsilon$ model was used in this study as the turbulence model because of the more realistic flame structures.

The k-ε model consists of the transport equations for k and ε The exact k equation is derived from scalar multiplication of the transport equation for the velocity fluctuation Du / Dt by the velocity fluctuation itself u:

$$
\rho\frac{Dk}{Dt} \equiv \underbrace{\rho\frac{\partial k}{\partial t}}_{L} + \underbrace{\rho U_j \frac{\partial k}{\partial x_j}}_{C} = \underbrace{\rho\overline{f_i u_i}}_{G} - \underbrace{\rho\overline{u_i u_j}\frac{\partial U_i}{\partial x_j}}_{P} - \underbrace{\mu\overline{\left(\frac{\partial u_i}{\partial x_j}\right)^2}}_{\rho\varepsilon} + \underbrace{\frac{\partial}{\partial x_j}\left(\mu\frac{\partial k}{\partial x_j} - \rho\overline{k u_j} - \overline{p u_i}\,\delta_{ij}\right)}_{D} \qquad (3)
$$

Equation ρDk/Dt describes the dynamics (and a budget) of the turbulent kinetic energy, where the terms have the following physical meanings: L - local change in time, C - convective transport, P - production of k ("of turbulence") by mean-flow deformation (work of turbulent stresses associated with the mean flow deformation, or transfer of the energy from the mean motion to the turbulent fluctuations by the action of Reynolds stresses),

Model Theoretical Background

Combustion formulation

The chemistry of ignition has been the subject of numerous studies (Cox, et al [10]; Fisch, et al [11]; Halstead, et al. "A Mathematical Model" [12]; Halstead, et al. "The Auto-ignition" [13]). There is now a general, although not precise, understanding of the hydrocarbon oxidation mechanism at pressure and temperature conditions relevant to the compression ignition of the diesel fuels.

The reaction mechanism used in this work for simulation of homogeneous charge compression ignition and of diesel fuel self-ignition has been developed along the lines of reaction scheme originally proposed for the study of auto-ignition phenomena in gasoline engines (Halstead, et al. "A Mathematical Model" [12]); Halstead, et al. "The Auto-ignition" [13]). In this reaction scheme, species that play a similar role in the ignition chemistry are combined and treated as a single entity.

In order to use the reaction mechanism within the framework of a multidimensional computation, reactions related to Propagation have been mass-balanced due to Schäpertöns and Lee.

The adaptation of the kinetic rate parameters is to predict self-ignition of diesel fuel as is also done by Theobald and Cheng.

NO_x Formulation

The reaction mechanism was expressed in terms of the extended Zeldovich mechanism [14]. In the literature different possibilities are suggested to represent the rate law for NO (Bogensperger [15]; Heywood [16]; Warnatz and Maas [17]).

In the present Combustion Model, an irreversible single-step reaction mechanism is used for the conversion of fuel, involving only stable molecules such as C_nH_m (as fuel), O_2, CO_2, H_2O and N_2. Hence, an approach is implemented based on these stable molecules in order to predict the thermal NO.

In addition, the characteristic times (Heywood [16]) for the formation of thermal NO is several orders of magnitude slower than the characteristic times of the combustion process.

Soot Formulation

The processes of particle formation and surface growth are taken to be related functions of the local fuel, soot nuclei concentration, and the predominating flame temperature governing the Arrhenius rate coefficient of the particle mass addition term respectively (Tatschl, et al [18]; Tesner, et al [19].).

Since in practical combustion devices, turbulent mixing predominantly influences the overall soot depletion rate, the particle oxidation process actually determines the soot emission level. It is modeled according to a hybrid chemical kinetic/turbulent mixing controlled rate expression, with the net oxidation rate governed by the slower of the two processes.

The soot oxidation source term is expressed in Magnussen and Hjertager [20].

Spray Formulation

The growth of an initial perturbation on a liquid surface is linked to its wavelength and to other physical and dynamic parameters of the injected fuel and the domain fluid [21].There are two break-up regimes, one for high velocities and one for low velocity Rayleigh type break-up.

The methods used in turbulent dispersion model is the stochastic dispersion method, which was employed by Gosman and Ioannidis [22]. In this method, the effects of turbulence on the spray particles are modeled by adding a fluctuating velocity to the mean gas velocity.

The Walljet1 has been used as the interaction model which is based in principle on the spray/wall impingement model of Naber and Reitz (1988) [23]. The concept is that under engine conditions, a vapor cushion is formed under the droplets, and that they rebound or slide along the walls. Since the wallfilm physics do not play an essential role within the wall interaction process; this model does not take into account the wallfilm physics.

The reflecting normal velocity component is calculated as a function of the droplet Weber number just before and after the impingement using an empirical correlation for the Weber number of the reflected drop. An empirical function has been derived from Wachters and Westerling [23].

For the jet regime, when the Weber number is bigger than a predefined value (We_C=80), it is assumed that an incident drop is reflected in the manner similar to the way a liquid jet would behave [23]. The droplet reflection velocity in this respect is calculated with the assumption that the magnitude is unchanged, and that only the reflection direction varies. The circumferential angle is determined by a probability distribution function, derived based on a two-dimensional potential flow jet conserving mass and momentum [24].

The droplet diameter after the impingement in both regimes is calculated as a function of Weber number currently distinguishing between the following Weber number criteria.

Journal of Fuel and Combustion
Vol. 1, No. 1, Sept. 2008

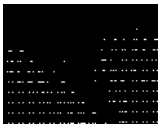

A Computational Study of the Effects of Combustion Chamber Geometries on Combustion Process and Emission in a DI Diesel Engine

S. Jafarmadar[*] and M. Khanbabazadeh[**]
Mechanical Engineering Department, Technical Faculty of Urmia University
(Receipt: 17/11/2007, Accepted: 06/11/2008)

A computational study aiming to investigate the effect of combustion chamber geometry on combustion process and emission has been carried out in a direct injection diesel engine. The combustion process and emission of three different combustion chamber geometries were considered, and combustion process behaviors such as variation of mean pressure, velocity, heat release rate, emission production and flame movement were revealed. The results also proved that the chamber shape has significant effects on the combustion and emission behaviors. They also showed that reentrant combustion chamber released less Soot and NO_x emissions because of intense swirl, tumble and low temperature combustion. Also it was known that depth of chamber is an effective parameter on NO_x and soot formation. The results of this model for cylindrical combustion chamber geometry were compared with the corresponding experimental data and proved to be good agreement. Generally it was found that the shape of Omega is the best selection for piston head, but it strongly needs strongly to match chamber geometry with spray characteristics.

Keywords: chamber geometry, modeling, emission, combustion process, swirl, tumble

Introduction

Recent advances in transportation industries need more efforts. DI engine designing and environmental legislations especially intensify this necessity. So achieving strict emission and efficiency standards is a vital goal. Many authors and engineers have tried to do this, and very useful ways have been offered to reach this purpose and advances have been made so far.

To reduce soot and NO_x emissions from diesel engines, important elements such as injection systems and charging systems are improved continually. To achieve the maximum benefit of such improvements, optimization of the combustion chamber geometry [1] is required. Because of the change in the chamber geometry, the changes of the in-cylinder air flow and the distribution of sprays can be predicted [1-3].

Konno at al [4] used an auxiliary combustion chamber with an additional injection nozzle and found that 10% of the total fuel injected in the auxiliary chamber at 15^0 of CA ATDC after the start of main injection can reduce smoke and fuel consumption without increasing NO_x.

Tow et al. [5] used an electronically controlled common rail unit injector to study the effects of single, double and triple injection schemes on NO_x and particulate emissions of a heavy duty DI diesel engine. They found that the benefit of double and triple injection strategies is the reduction in NO_x without increasing the particulate when the injection timing is retarded.

Bai. Lin [6] from Nippon Institute of technology developed a multi-impingement-wall head (MIW head) to obtain a three-dimensional diffusion spray for improving the combustion and performance of a DI diesel engine. Their study showed that the reentrant type of combustion chamber with projection and cutouts has a better fuel consumption and produces lower harmful exhaust gases (HC, NO_x and smoke) than those of other NICS-MH engines.

Long. Zhang et al [7] carried out an experimental study in an optically accessible, naturally aspirated DI diesel engine fitted with an extended piston to investigate the effect of combustion chamber geometry on combustion process behaviors. They developed 3 pistons with different chamber shapes for a 2 valves NA DI Diesel engine. They used the cross-correlation method for measuring the flame velocity described in detail by Shioji [8] and Yamaguchi [9]. They also correlated the smoke changes under the same conditions as the combustion visualization with the flame behaviors in order to understand the crucial relationship between them. Their study showed that the flame distribution inside and outside the chamber is considerably affected by the chamber geometry, the reentrant chamber prevents the flame from spreading over the squish region. They also similarly found that the particular reentrant chamber with a pronounced center cone has shown larger flame velocity than the dish chamber during expansion period, and that the velocity is smaller in the squish region.

Many other enhanced efforts have been done based on the CFD method [2], [3] to predict how the geometry of chamber can influence combustion process as well as engine exhaust gases. However, there is a long way to reach the desired standard. This work is an effort along the same endeavor too.

[*] Assistant professors- Correspondent author (Email: S.Jafarmadar@mail.urmia.ac.ir)
[**] Graduate student (Email: mojtaba_khanbabazadeh@yahoo.com)